(4)/cw/IN/38

2001 NASA/ASEE SUMMER FACULTY FELLOWSHIP PROGRAM

JOHN F. KENNEDY SPACE CENTER
UNIVERSITY OF CENTRAL FLORIDA

Assessing the Rayleigh Intensity Remote Leak Detection Technique

Dr. Sandra Clements
Visiting Assistant Professor
Physics and Space Sciences
Florida Institute of Technology
Christopher Davis

ABSTRACT

Remote sensing technologies are being considered for efficient, low cost gas leak detection. An exploratory project to identify and evaluate remote sensing technologies for application to gas leak detection is underway. During Phase 1 of the project, completed last year, eleven specific techniques were identified for further study. One of these, the Rayleigh Intensity technique, would make use of changes in the light scattered off of gas molecules to detect and locate a leak. During the 10-week Summer Faculty Fellowship Program, the scatter of light off of gas molecules was investigated. The influence of light scattered off of aerosols suspended in the atmosphere was also examined to determine if this would adversely affect leak detection. Results of this study indicate that in unconditioned air, it will be difficult, though perhaps not impossible, to distinguish between a gas leak and natural variations in the aerosol content of the air. Because information about the particle size distribution in clean room environments is incomplete, the applicability in clean rooms is uncertain though more promising than in unconditioned environments. It is suggested that problems caused by aerosols may be overcome by using the Rayleigh Intensity technique in combination with another remote sensing technique, the Rayleigh Doppler technique.

Sandra Clements

1. INTRODUCTION

Detecting and locating gas leaks is a costly endeavor critical to the safety and success of launching vehicles into space. Remote sensing technologies are being considered as replacement for in situ techniques with the goal of dramatically reducing the cost of detecting gas leaks by an order of magnitude or more. During Phase 1 of the Remote Leak Detection project, eleven remote sensing technologies were identified for further study (private communication from Glenn Sellars and Danli Wang, Florida Space Institute, Kennedy Space Center, Florida). The level of theoretical and experimental development of each technology was assessed for its applicability to remote leak detection. The specific goal of the Remote Leak Detection project is to identify remote sensing techniques that will locate hydrogen and helium leaks into air. The two gases, hydrogen and helium, were chosen because of their importance in verification and normal operations of launch systems. These gases are also among the most challenging to detect.

One of the eleven possible remote leak detection techniques, the Rayleigh Intensity technique, was investigated during the 10-week Summer Faculty Fellowship Program. The results of that investigation are described here.

2. THE RAYLEIGH INTENSITY TECHNIQUE

With the Rayleigh Intensity technique, a laser would be directed toward the site being monitored for gas leaks. The laser light would scatter off of air molecules (and particulates) and this scattered light would be detected. In order for this technique to be viable for leak detection, the intensity of scattered light with and without a leak would need to differ. Because this technique involves the scatter of electromagnetic radiation off of small particles, a theory describing such scatter will be examined.

2.1. Mie Theory and the Scatter of Electromagnetic Radiation

Mie theory [1] was developed to describe the scattering of electromagnetic radiation by spherical particles. The derivation of Mie scattering theory involves finding the solutions of Maxwell's equations that describe the electromagnetic field resulting when a plane, monochromatic wave is incident on a spherical particle immersed in a homogeneous, isotropic medium. Because the solution consists of an infinite, though converging, sum of complicated terms involving Legendre functions and Bessel functions [2], computer programs are used to solve it numerically.

When the particle radius (a) is small compared to the wavelength (λ) of incident radiation ($a \leq \sim 0.1\lambda$) the intensity (I) of scattered light satisfies Rayleigh's Law ($I \propto 1/\lambda^4$). For larger radii, the scattered intensity has a flatter dependence on wavelength ($I \propto 1/\lambda^{0\text{-}2}$). In the visible region of the spectrum, Rayleigh scattering occurs from air molecules and small aerosol particles (sea salt and atmospheric dust condensation nuclei, etc.) whereas Mie scattering occurs from larger aerosol particles (dust, pollen, water droplets, etc.).

Rayleigh's Law, given below, describes the scattered intensity in the small particle limit [3].

$$I = I_0 \frac{8\pi^2 a^6}{r^2 \lambda^4} \left(\frac{(n^2 - 1)}{(n^2 + 2)} \right)^2 \left(1 + \cos^2 \theta\right) \qquad \text{Rayleigh's Law}$$

The functional dependence of the scattered intensity on the particle's refractive index n, the wavelength □ of the incident radiation, the scattering angle □, and the particle size a will be examined in turn.

2.2. Index of Refraction

It is because the intensity is proportional to $((n^2 - 1)/(n^2 + 2))^2$ and the three gases of interest have very different values for this quantity that the Rayleigh Intensity method is considered a possible leak detection technique. The values for n and $((n^2 - 1)/(n^2 + 2))^2$ for the three gases of interest are given in the table below. Note that the intensity due to Rayleigh scattering in air is expected to be about 70 times greater than the intensity due to scattering in helium given that all other conditions are the same.

Gas	n	$\left((n^2-1)/(n^2+2)\right)^2$
Air	1.000274	3.34×10^{-8}
Hydrogen	1.000122	6.61×10^{-9}
Helium	1.000033	4.84×10^{-10}

In the general theory, the index of refraction can be complex and is expressed $n = n_r + i\, n_i$. The real term is the familiar $n_r = c/v$ where c is the speed of electromagnetic radiation in vacuum and v is its speed in the medium of interest. The imaginary term n_i is non-zero for absorbing materials. Values for the index of refraction of aerosols typically found in the atmosphere [4, 5] are given below.

Medium	Index of refraction
Water	1.333
Inorganic materials	1.45 – 1.6
Crystalline aerosols	1.48 – 1.64
Soot aggregates	1.56 + 0.47i

2.3. Wavelength

In the Rayleigh regime, the intensity of scattered radiation from small particles falls off like $1/\lambda^4$. Thus short wavelength radiation is scattered more efficiently than long wavelength radiation. In the Mie regime, the wavelength dependence is flatter.

The influence of particle size on the type of scattering that occurs is illustrated beautifully in nature every day. Sunlight consists of all the colors of the rainbow – red, orange, yellow, green, blue, and violet. Viewed together, these different colors are perceived as white light. When the sun's light travels through the atmosphere, it scatters off of molecules and aerosols. Because air molecules are very tiny ($a \sim 0.00015\mu m$), they scatter the shorter wavelength blue light ($\lambda \sim 0.4\mu m$) more readily than the longer wavelength red light ($\lambda \sim 0.7\mu m$). Thus when you look at the clear sky in a direction other than toward the sun, you are observing blue light that originated with the sun but that was scattered toward you by air molecules.

Clouds contain water droplets that are large relative to the wavelength of visible light. The water droplets scatter all wavelengths of the incident sunlight approximately equally. When you look at a cloud, you see the combined scattered light from many water molecules. This scattered light consists of approximately equal quantities of all the different colors of light and thus our mind perceives the cloud to be white. The same is true of fog and smoke.

The sun appears redder when it is near the horizon than it does when it is higher in the sky. This is because when the sun is low on the horizon, its light must travel through a longer path length of atmosphere than when it is higher in the sky. By the time the sun's light reached the observer, the shorter wavelengths (violet, blue, green) of light have been scattered out, leaving only the longer wavelengths (reds, oranges, yellow).

2.4. Scattering Angle and Particle Size

Rayleigh scattering varies with scattering angle, $I \propto 1 + \cos^2\theta$. Thus, the scattered radiation has its greatest intensity in the forward ($\theta = 0°$) and backward ($\theta = 180°$) directions. The forward direction is the

direction of propagation of the incident wave. The minimum intensity is found perpendicular to the direction the incident wave was traveling. This scattered radiation is polarized with the greatest polarization also occurring perpendicular to the direction of propagation of the incident wave.

Mie scattering is a more complicated function of scattering angle. The scattered intensity becomes more and more strongly forward scattered as the particle size increases. Furthermore, the angular dependence of the scattering pattern varies as the particle size varies. The dependence of polarization on angle also changes with particle size. Thus the scattered intensity from an ensemble of aerosol particles of varying sizes will be less polarized than the scattered intensity from molecules of air. If you put on Polaroid sunglasses that block out the light polarized in one direction, the intensity of the blue sky will diminish more than the intensity of the white clouds.

3. INSIGHTS FROM RUNS OF A MIE SCATTERING CODE

The simulated results in this section were obtained by running the Mie scattering code of Barber and Hill [6] for spherical particles. This Mie code was used to compute the intensity as a function of size parameter $q = 2\pi a/\lambda$ for the case of backscattering $\theta = 180°$ and parallel incident polarization. In the case of backscattering, the results are the same for the perpendicular incident polarization as for parallel incident polarization. From these results, the relationship between backscattered intensity and wavelength can be computed for any particle size. Figure 1 shows this relationship for a particle of radius $a = 0.0001\square m$, approximately the size of an air molecule.

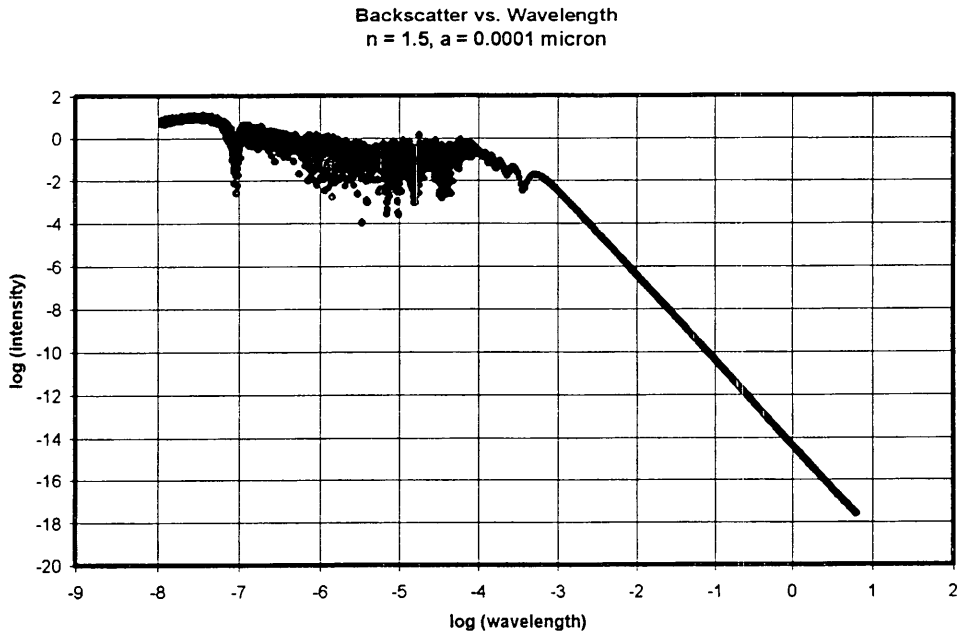

Figure 1: Backscatter as a function of wavelength for a particle with radius a = 0.0001□m.

In Figure 1, the intensity follows the Rayleigh relationship ($I \propto \lambda^{-4}$) when the wavelength is large compared to the radius of the particle or, equivalently, the radius small relative to the wavelength ($a < \sim 0.1\lambda$, $\log q < 0$ or q < 1). For larger particles ($a > \sim 0.1\lambda$, $\log q > 0$ or q > 1), the intensity-wavelength relationship is much flatter as expected for Mie scatter. For an air molecule with a radius of ~0.0001□m, the intensity follows Rayleigh's Law in the visible part of the spectrum ($0.40\mu m < \lambda < 0.70\mu m$, $-0.40 < \log\lambda < -0.15$), scattering blue light much more readily than red light.

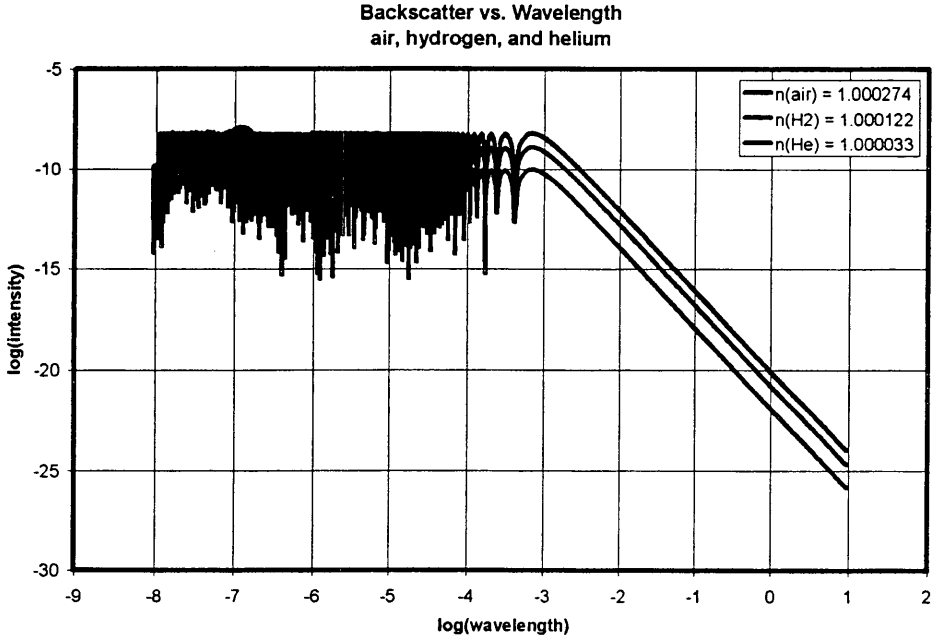

Figure 2: Backscattered intensity as a function of wavelength for air, hydrogen, and helium.

Shown in Figure 2 are the results from the Mie scattering code using the refractive indices for air, hydrogen, and helium. Note that in the visible part of the spectrum, the intensity indeed increases with increasing index of refraction as expected from the relationship $I \propto ((n^2-1)/(n^2+2))^2$. Comparing the intensity for air and the intensity for helium using this relationship gives the following.

$$\frac{I(n_{air}=1.000274)}{I(n_{He}=1.000033)}=\left(\frac{(n_{air}^2-1)/(n_{air}^2+2)}{(n_{He}^2-1)/(n_{He}^2+2)}\right)^2=\left(\frac{(1.000274^2-1)/(1.000274^2+2)}{(1.000033^2-1)/(1.000033^2+2)}\right)^2=68.9$$

The Mie scattering code gives the same ratio in the Rayleigh regime. For example, at $\lambda = 0.550\mu m$, the code gives the following simulated result.

$$\frac{I(n_{air}=1.000274)}{I(n_{He}=1.000033)}=\left(\frac{9.44976\times10^{-20}}{1.37126\times10^{-21}}\right)=68.9$$

In Figure 3, the results from the Mie scattering code for various aerosol refractive indices are shown. The five curves in this figure are for $n = 1.33$, 1.5, 1.7, $1.5+0.1i$, and $1.5+0.5i$. These five refractive indices cover the range of values expected for aerosol particles in the atmosphere [4, 5]. The first value ($n = 1.33$) is appropriate for water droplets in clouds and fog. The value $n = 1.5$ is commonly used in simulations for aerosol particles.

Comparing the curves for the real refractive indices reveals that the larger the refractive index, the steeper the slope in the Mie regime. Thus particulates with larger indices of refraction will scatter blue light slightly more readily than red light even in the Mie regime. Clouds composed of water molecules with small refractive indices ($n = 1.33$) scatter rather independently of wavelength in the Mie regime. Clouds therefore appear white.

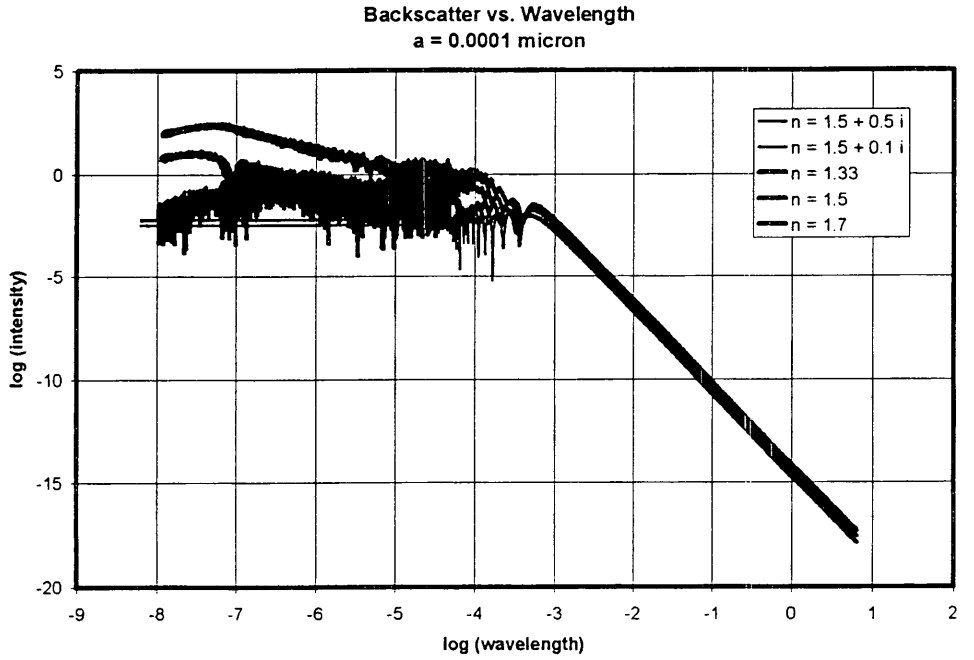

Figure 3: Relationship between backscattered intensity and wavelength for particles of various refractive indices.

4. PARTICLE SIZE DISTRIBUTION

Increasing the particle size by a factor of ten has the effect of shifting the curve horizontally toward higher wavelengths by a factor of ten. Particles smaller than ~0.1μm contribute to Rayleigh scattering in the visible part of the spectrum (*-0.40 < log λ < -0.15*), whereas those with larger radii contribute to Mie scattering. The particle size distribution for the medium through which the radiation is traveling is required in order to determine the total backscattered intensity

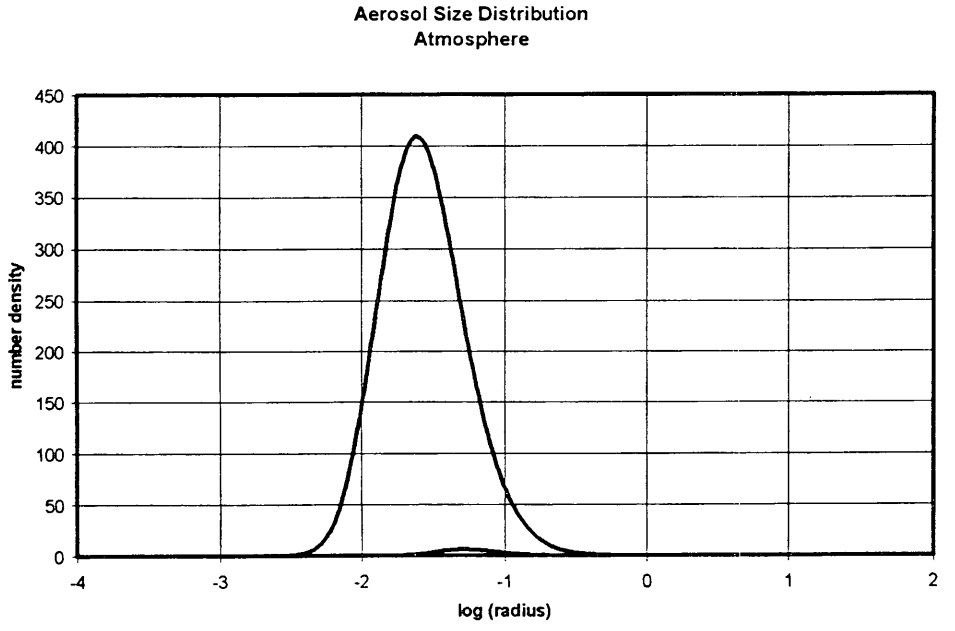

fr om an ensemble of particles of various sizes.

Figure 4: Particle Size Distribution for Continental Aerosols.
The particle size distribution is the number density of particles within a given range of sizes. This is a difficult entity to pin down. For outdoor applications, the particle size distribution will change due to the influence of weather, human activity (fires, for example), and season (springtime pollen, for example). For clean room environments, it is controlled within a range of particle sizes though not fully defined for all particle sizes.

Figure 4 shows the particle size distribution for continental aerosols [7]. This particle size distribution was used to compute the relationship between backscattered intensity and wavelength for the ensemble of particles in the air shown in Figure 5. Similar simulations were run using the particle size distribution in maritime [5] and clean room [8] conditions. The distributions for these latter two cases lack information about the number density of small particles and thus results based on these distributions are uncertain.

5. SIMULATIONS OF THE BACKSCATTERED INTENSITY FROM AN ENSEMBLE OF PARTICLES

To determine the backscattered intensity from an ensemble of particles, the backscattered intensity as a function of wavelength is determined for each particle size. Each of these is multiplied by the number density of particles having that size. At each wavelength, the total intensity contributed by all particles of each size is then summed to give the ensemble, backscattered intensity as a function of wavelength.

The ensemble result for unconditioned air having the continental aerosol content of Figure 4 is shown in Figure 5. It was obtained by summing the contribution from 600 particle sizes ranging over 6 orders of magnitude from $a = 0.0001\mu m$ to $a = 100\mu m$. The ensemble result was computed to be valid only for wavelengths within the range $-2 < \log \lambda < 1$. Only this wavelength range is shown in Figure 5. In this wavelength range, there is a contribution to the backscattered intensity from all particles sizes. The visible part of the spectrum ($-0.4 < \log \lambda < -0.15$) is included in the valid range.

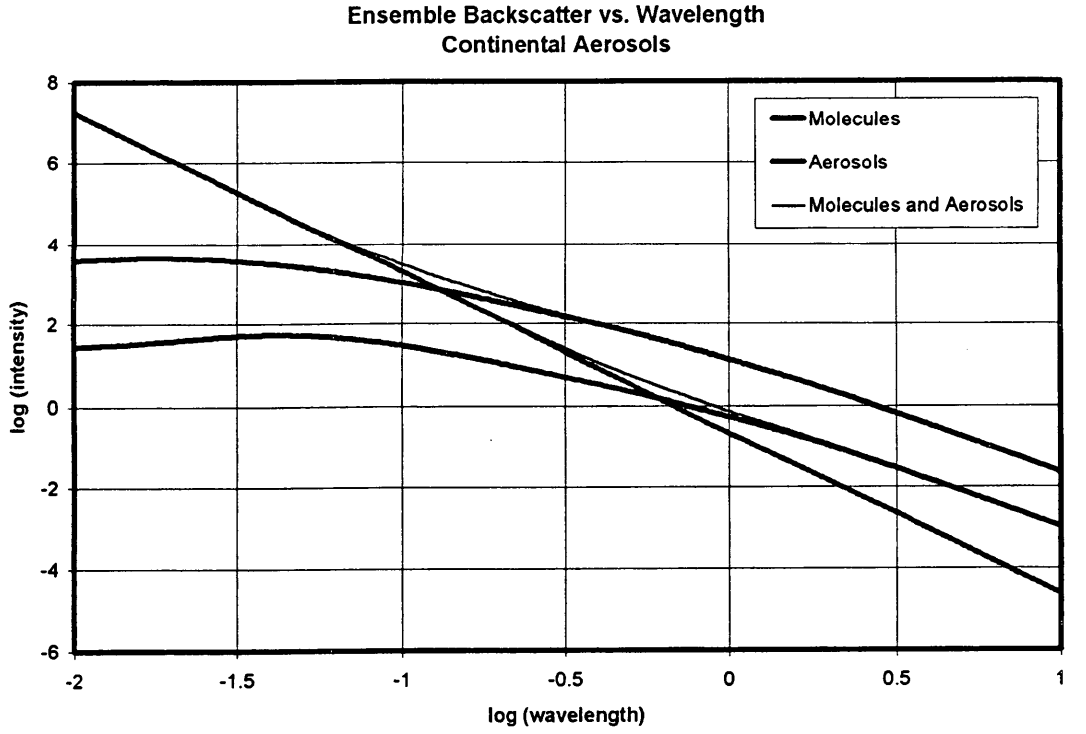

Figure 5: The backscattered intensity as a function of wavelength computed using the continental aerosol particle size distribution.

The thick black curve shows the contribution from the air molecules alone, without aerosol particles. A radius of 0.00015□m was used for the size of an air molecule and a number density of 2.5×10^{19} molecules/cm^3 was used for the density of air molecules in the atmosphere. The molecules exhibit Rayleigh scatter ($I \propto \lambda^{-4}$) over the valid wavelength range.

The gray curves show the contribution from the aerosol particles in the continental atmosphere. The upper curve represents the result when the atmospheric aerosol content is high and the lower curve represents the result when the aerosol content is low. The thin black curves represent the ensemble results for which both molecules and aerosol particles contribute.

When the aerosol content is low, the Rayleigh backscatter from molecules equals the backscatter from aerosols at a wavelength of ~0.6□m (*log* λ ~ *-0.22*) in the visible part of the spectrum. Furthermore, the total backscatter from molecules and aerosols (the lower thin black curve) is dominated by Rayleigh scatter from molecules for wavelengths less than ~0.288□m (*log* λ ~ *-0.54*). Unfortunately, this is in the ultraviolet, not visible, part of the spectrum.

When the aerosol content is high, Rayleigh backscatter from molecules equals the backscatter from aerosols at the ultraviolet wavelength of ~0.132□m (*log* λ ~ *-0.88*). The total backscatter from molecules and aerosols (the upper thin black curve) is dominated by Rayleigh scatter from molecules for wavelengths less than ~0.1□m (*log* λ ~ *-1*). At all visible wavelengths, the total backscatter is dominated by the scatter off of aerosol particles.

Note that for wavelengths less than ~0.1□m, variations in aerosol content have no significant effect on the total backscattered radiation. Unfortunately, the atmosphere is not transparent to these wavelengths and thus the Rayleigh Intensity technique would not work for detecting gas leaks in air.

Because the contribution from aerosols dominates the backscattered intensity when the aerosol content is high, a change in the backscattered intensity due to the addition of a leaking gas is unlikely to result in a significant variation in the backscattered intensity. It may be possible, however, to detect a significant variation in the backscattered intensity if the leaking gas causes a significant displacement of aerosols near the site of the leak. It will be difficult to distinguish between variations due to leaks and variations due to naturally changing aerosol content however. Figure 5 shows that the expected variations in the aerosol content of continental air would result in an order of magnitude variation in the total backscattered radiation from a laser operating in the visible part of the spectrum. Such variations in the aerosol content may mask variations due to hydrogen or helium leaks. A possible solution may be to scan the laser over a region and look for localized reductions in the backscattered intensity.

Because KSC and CCAFS are on the coast, simulations were run using the particle size distribution for maritime aerosols. Unfortunately, the lack of information on the small particle size distribution leads to uncertain results for the backscattered intensity. If one makes the assumption that the size distribution for the smaller particles is similar to that for continental air, the conclusions found for continental air would hold for maritime air as well.

Finally, simulations were run using the particle size distribution for clean room conditions. Again, the particle size distribution for these conditions is incomplete, failing to show the number density of the smaller particles. The results for clean room conditions are therefore uncertain. According to Stowers [8], the filters that condition the air for clean rooms have a harder time filtering particles with radii ~0.25□m than either larger or smaller particles. Thus, it may be that the number density of smaller particles is lower than for the same sized particles in unconditioned air. If the particle size distribution of Stowers [8] can be extrapolated to particles with radius *a = 0.01□m*, simulations indicate the backscattered intensity for Class 1 – 1000 clean rooms would be dominated by scatter off of molecules at visible wavelengths and thus the Rayleigh Intensity technique might be viable in those conditions. It might even be viable in Class 10,000 clean rooms, since the molecular contribution to the backscatter is significant in those conditions as well.

6. COMBINED RAYLEIGH INTENSITY AND RAYLEIGH DOPPLER TECHNIQUES

Even if the backscattered intensity is dominated by scattering off of aerosols, it should be possible to determine the contribution from Rayleigh scattering off of molecules using the Rayleigh Doppler technique. A high technology company, Ophir Corporation, is developing what it calls a Rayleigh/Mie Lidar system to replace the pitot tubes on aircraft and thus reduce their radar cross-sections. This technique makes use of the backscattered intensity from a laser that samples the air to determine things such as airspeed, pressure, and temperature. Both the backscattered Rayleigh signal from molecules and the backscattered signal from aerosols are detected.

In an experiment carried out in a Denver, Colorado laboratory (altitude ~5300ft), a laser with a wavelength of 852nm (0.852μm) was used to produce the Ophir Corporation's experimental results shown in Figure 6 (private communication from Martin O'Brien, Ophir Corporation, Denver, CO). This wavelength is in the infrared part of the spectrum. The random motion of the molecules Doppler shifts the backscattered radiation, thus spreading the signal out over a range of frequencies centered on the frequency of the laser. The greater the average speed of the particles, the broader the peak will be.

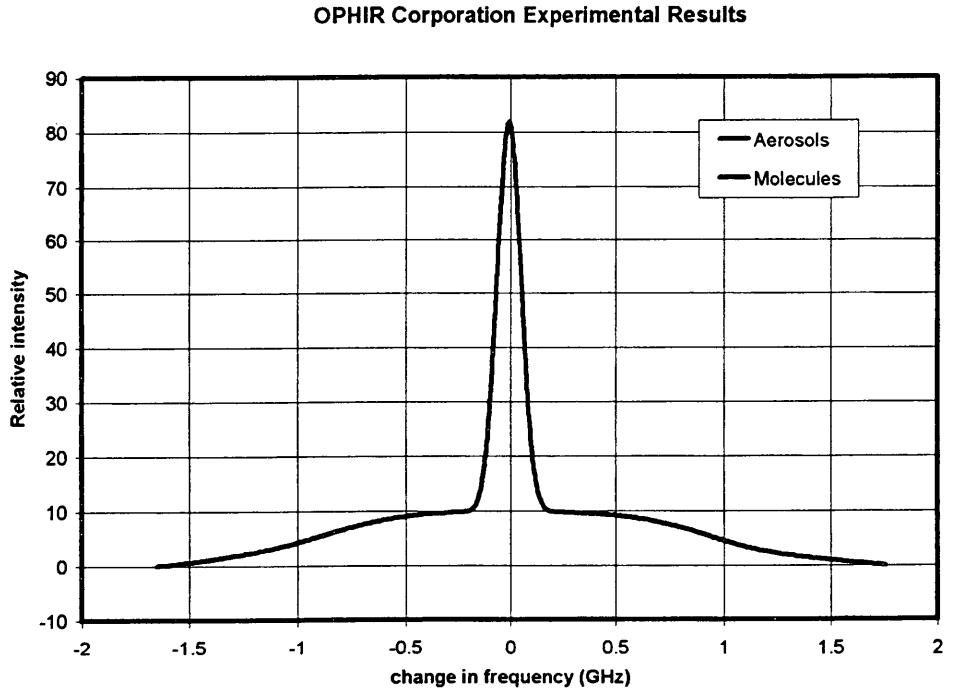

Figure 6: Results from an Ophir Corporation experiment for their Rayleigh/Mie Lidar system. (See http://www.ophir.com/rayleigh_mie_optical_data.htm for more information)

Figure 6 shows the backscattered intensity as a function of the shift in frequency. The curve has two components. The sharp, narrow peak is due to backscatter off of the larger, slower aerosol particles. The shallow, broad peak is due to backscatter off of the smaller, faster air molecules. Thus, despite the apparent strength of the aerosol component, the Rayleigh component can be identified. Integrating under the two peaks gives the backscattered intensity due to each component. When this is done, it turns out that the Rayleigh backscattered intensity from molecules is about twice the backscattered intensity from aerosols. It is interesting that at infrared wavelengths, the integrated Rayleigh signal from molecules is stronger than the integrated signal from aerosols. Extrapolating to half the experimental wavelength indicates that at 0.426□m, the backscattered intensity due to molecules would be anywhere from 4 – 16 times the backscattered intensity due to aerosols. The Ophir Corporation experimental results indicate that it is possible to distinguish between molecular and aerosol backscatter and thus it may be possible to monitor the molecular backscatter for changes due to gas leaks even when there is strong aerosol backscatter.

7. CONCLUSIONS

Application of the Rayleigh Intensity technique toward detection of hydrogen and helium leaks will be problematic in unconditioned (outdoor) air. When the aerosol content in the atmosphere is high, the leaking gas itself will not result in significant variations in the backscattered radiation since the backscattered radiation is dominated by scattering from aerosol particles. However, the leaking gas may displace aerosol particles near the leak and thus result in a decrease in the backscattered intensity. The normal variation of aerosol content in the atmosphere will also result in significant variations in the backscattered intensity of light. To distinguish this normal variation from that due to a leak will be challenging. Perhaps scanning the laser over an area and noting localized decreases in the backscattered radiation would make it possible to locate a leak.

Because the particle size distribution for clean room conditions is incomplete, it is unclear whether the Rayleigh Intensity technique would be a viable technique in those conditions. If the particle size distribution of smaller particles can be considered an extrapolation of the large particle distribution to a radius of 0.01 □m, simulations indicate the technique will be viable for Class 1 – 1000 clean rooms at all visible wavelengths and for Class 10,000 clean rooms for wavelengths shorter than ~0.5□m. If the particle size distribution of smaller particles is the same as for unconditioned air, then the conclusions for unconditioned air apply. Further work to pin down the particle size distribution for small particles is indicated to eliminate uncertainties caused by the incomplete data available.

Experimental evidence has been presented indicating that it is possible to isolate the molecular contribution to the backscattered intensity from the aerosol contribution using another remote sensing technique, the Rayleigh Doppler technique. The variation in the Rayleigh scatter by molecules could then be monitored for changes due to leaks. It would be beneficial to determine the range of ratios of $I_{Rayleigh}/I_{Mie}$ over which it would be possible to distinguish between the molecular and aerosol components.

REFERENCES

[1] Mie, G, *Ann. d. Physik (4)*, 25, (1908), 377

[2] Born, Max and Wolf, Emil, *Principles of Optics. Electromagnetic Theory of Propagation, Interference and Diffraction of Light, 5th edition*, Pergamon Press, Oxford, (1975)

[3] Lang, Kenneth R., *Astrophysical Formulae*, Springer-Verlag, New York, (1980)

[4] Mészáros, Ern□, *Fundamentals of Atmospheric Aerosol Chemistry*, Akadémiai Kiadó, Budapest, (1999)

[5] McCartney, Earl J., *Optics of the Atmosphere. Scattering by Molecules and Particles*, John Wiley & Sons, New York. (1976)

[6] Barber, P. W. and Hill, S. C., *Light Scattering by Particles. Computational Methods*, World Scientific, New Jersey, (1990)

[7] Israël, H. and Israël, G. W., *Trace Elements in the Atmosphere*, Ann Arbor Science Publishers, Inc., Ann Arbor, Michigan, (1974)

[8] Stowers, Irving F., *SPIE*, 3782, (1999), 525-530